

## Effects of Precursor on the Morphology and Size of ZrO<sub>2</sub> Nanoparticles, Synthesized by Sol-gel Method in Non-aqueous Medium

Mohammed Rafiq Hussain Siddiqui<sup>a\*</sup>, Abdulaziz Ibrahim Al-Wassil<sup>a</sup>,

Abdullah Mohammed Al-Otaibi<sup>b</sup>, Refaat Mohamad Mahfouz<sup>a</sup>

<sup>a</sup>Department of Chemistry, College of Science, King Saud University,  
Riyadh 11451, PO BOX 2455, Kingdom of Saudi Arabia

<sup>b</sup>The National Program for Advanced Materials and Building Systems,  
King Abdulaziz City for Science and Technology, Saudi Arabia

Received: October 11, 2011; Revised: July 15, 2012

Pure zirconium oxide (ZrO<sub>2</sub>) nanoparticles with diameters 10-25 nm were synthesized from ZrOCl<sub>2</sub>·8H<sub>2</sub>O and Zr(SO<sub>4</sub>)<sub>2</sub>·H<sub>2</sub>O with benzyl alcohol as non-aqueous solvent medium using sol-gel method. Sodium lauryl sulfate was added as surfactants to control the particle size. The synthesized ZrO<sub>2</sub> nanoparticles have a mixture of tetragonal and monoclinic structure. The XRD showed the purity of obtained ZrO<sub>2</sub> nanoparticles with tetragonal and monoclinic phase and the crystallite size for ZrOCl<sub>2</sub>·8H<sub>2</sub>O precursor was estimated to be 18.1 nm and that from Zr(SO<sub>4</sub>)<sub>2</sub>·H<sub>2</sub>O was 9.7 nm. The transmission electron microscopy and scanning electron microscopic studies also shows different sizes of nanoparticles and different morphology depending on the precursor used for the synthesis of ZrO<sub>2</sub> nanoparticles.

**Keywords:** *zirconia, nanoparticles, electron microscopy, precursor and morphology*

### 1. Introduction

Pure zirconia ZrO<sub>2</sub> exhibits three polymorphs of monoclinic, tetragonal and cubic symmetries. The monoclinic phase is stable at room temperature and transforms to the tetragonal phase at 1170 °C during heating, while this phase transforms to the cubic one at 2370 °C<sup>1,2</sup>. Both transformations are reversible on cooling, although the t → m transition occurs at a lower temperature (about 950 °C). This martensitic transformation, which has been extensively studied, is the basis of the “transformation toughening mechanism” exhibited by zirconia-based materials<sup>3</sup>. About 95% of ferrules used in optical fiber connectors are made of zirconia<sup>3</sup>. Zirconia has unique physical and chemical properties e.g. excellent thermal and chemical stability, high strength and fracture toughness, low thermal conductivity, high corrosion resistance. Both acidic and basic properties of zirconia have been widely used in the fields of structural materials, thermal barrier coatings, oxygen sensors, fuel cells, catalysts and catalytic supports, a possible high dielectric constant material for large scale integrated circuits, and as a gate dielectric in metal oxide-semiconductor (MOS) devices<sup>4-6</sup>. Ultrafine zirconia particles have been synthesized via various methods such as sol-gel processing<sup>7-9</sup>, chemical vapor synthesis<sup>10</sup>, precipitation from inorganic salt solutions<sup>11,12</sup>, microwave plasma synthesis<sup>13</sup>, inert gas condensation<sup>14</sup>, combustion synthesis<sup>15</sup>, ultrasonically assisted hydrothermal synthesis<sup>16</sup> and laser ablation<sup>17</sup>. In this study we report the synthesis of

zirconia nanoparticles synthesized by sol-gel technique in non aqueous medium.

### 2. Material and Methods

To 1 mmol ZrOCl<sub>2</sub>·8H<sub>2</sub>O or Zr(SO<sub>4</sub>)<sub>2</sub>·H<sub>2</sub>O, 2 mmol of benzyl alcohol was added drop-wise, to form a gel. This was followed by the addition of 2 mmol of sodium lauryl sulfate with constant stirring. The product was dried at a temperature of 200 °C for 5 hours and calcined at temperature 600 °C for 5 hours; (Figure 7) shows the method of preparation of ZrO<sub>2</sub> nanoparticles. The samples synthesized were characterized by X-ray powder diffraction (XRD) using (Altima IV Rigaku, X-ray diffractometer and CuKα as X-ray source) transmission electron microscopy was done on (JEN2100F, JEOL, TEM) and scanning electron microscopic studies were carried out on (NNL 200, FEI, SEM) and Perkin-Elmer 1000 FT-IR spectrophotometer.

### 3. Results and Discussion

#### 3.1. FT-IR spectra

The FT-IR spectra of all the samples were similar. The IR spectrum of typical samples, show a strong broad absorption centered around 3413 cm<sup>-1</sup>, three sharp absorption bands at about 1630, 1352, and 1044 cm<sup>-1</sup>, and two weak absorption bands at 580 and 454 cm<sup>-1</sup>. The bands at about 508 and 493 cm<sup>-1</sup> correspond to Zr–O vibration of tetragonal structure<sup>18</sup>. The absorption band located around

\*e-mail: rafiqs@ksu.edu.sa

3413 cm<sup>-1</sup> is associated with the O–H stretching vibration of adsorbed water and hydroxyl group, while the absorption band at 1630 cm<sup>-1</sup> is due to the bending mode of associated water<sup>19</sup>. The observation of a strong broad absorption at 3400 and sharp absorption band at 1044 cm<sup>-1</sup> implied that the hydrated molecules could be in several different energetically bonding states.

### 3.2. X-ray diffraction patterns

The XRD patterns of the ZrO<sub>2</sub> samples calcined at 600 °C for 5 hours for both precursors ZrOCl<sub>2</sub>·8H<sub>2</sub>O and Zr(SO<sub>4</sub>)<sub>2</sub>·H<sub>2</sub>O were similar. The XRD pattern obtained from ZrOCl<sub>2</sub>·8H<sub>2</sub>O and Zr(SO<sub>4</sub>)<sub>2</sub>·H<sub>2</sub>O are shown in Figures 1, 2.

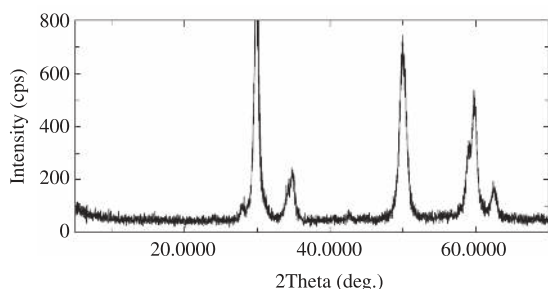


**Figure 1.** XRD of zirconia nanoparticles synthesized by sol-gel method using ZrOCl<sub>2</sub>·8H<sub>2</sub>O as precursor.

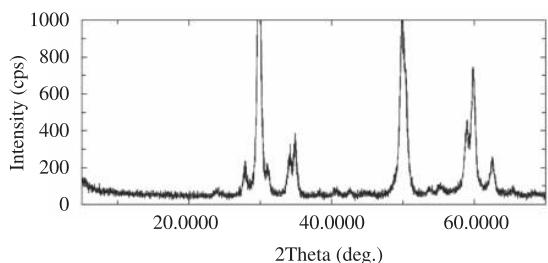


**Figure 2.** XRD of zirconia nanoparticles synthesized by sol-gel method using Zr(SO<sub>4</sub>)<sub>2</sub>·H<sub>2</sub>O as precursor.

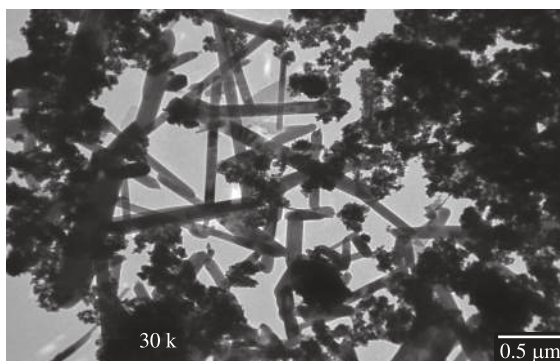


**Figure 3.** TEM image of zirconia nanoparticles synthesized by sol-gel method using ZrOCl<sub>2</sub>·8H<sub>2</sub>O as precursor.

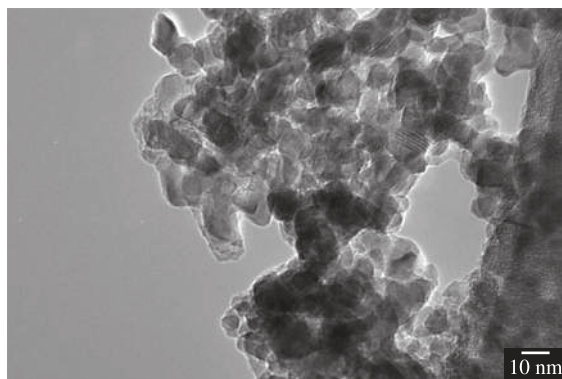
Pure ZrO<sub>2</sub> shows both monoclinic ( $\theta = 27$  and  $31.1^\circ$ ) and tetragonal ( $\theta = 30^\circ$ ,  $34.9$ ,  $50$  and  $60^\circ$ ) phase. Scherrer equation was used to calculate the crystallite sizes for the ZrO<sub>2</sub> samples and the crystallite size for ZrOCl<sub>2</sub>·8H<sub>2</sub>O precursor was estimated to be 18.1 nm and that from Zr(SO<sub>4</sub>)<sub>2</sub>·H<sub>2</sub>O was 9.7 nm. It should be noted that the precursor has a significant effect on the resulting ZrO<sub>2</sub> crystallite size.

### 3.3. TEM, SEM and AFM image

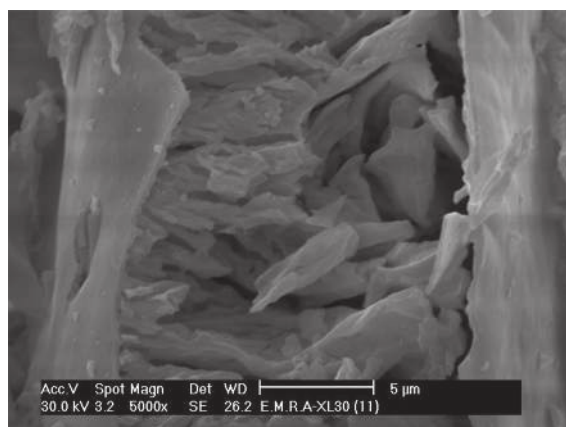
The particle composition was also studied by TEM and SEM and the images are shown in Figures 3-6. Figure 3 shows TEM image of zirconia nanoparticles synthesized by sol-gel method using ZrOCl<sub>2</sub>·8H<sub>2</sub>O. The estimated diameters of nanoparticles were found to be 25 nm. It could be seen that the particles has two distinct shapes. One is rod-shaped or nanotubes which are long narrow and appear closed at both ends and the other are much smaller and clustered in a flower shape. Probably these small clusters grow to give the nanotubes observed in the TEM image.

Figure 4 shows TEM image of zirconia nanoparticles synthesized by sol-gel method using Zr(SO<sub>4</sub>)<sub>2</sub>·H<sub>2</sub>O, it could be seen that the particles are uniform and spherical and the average particle size calculated was about 10 nm. There is slight difference in the size of particles obtained from TEM compared to the crystallite size obtained by XRD. This can be attributed to differences of accuracy of measurements of the two different techniques coupled with the fact that the particles obtained from ZrOCl<sub>2</sub>·8H<sub>2</sub>O precursor are of two different types and the size difference between these particles is fairly significant. The XRD pattern cannot see these minor differences that can be observed by TEM technique.

Figure 5, shows the SEM image of ZrO<sub>2</sub> obtained from ZrOCl<sub>2</sub>·8H<sub>2</sub>O precursor and it appears to have a very ill-defined shape. The image appears to show particles like a broken rib cage. Due to this ill-defined morphology, it is possible that the SEM does not give a clear idea of formation of nanoparticles in this case. However, the morphology for the ZrO<sub>2</sub> obtained from Zr(SO<sub>4</sub>)<sub>2</sub>·H<sub>2</sub>O precursor is very different. Figure 6, shows the SEM image of ZrO<sub>2</sub> obtained



**Figure 4.** TEM image of zirconia nanoparticles synthesized by sol-gel method using Zr(SO<sub>4</sub>)<sub>2</sub>·H<sub>2</sub>O as precursor.



**Figure 5.** SEM image of zirconia nanoparticles synthesized by sol-gel method  $\text{ZrOCl}_2 \cdot 8\text{H}_2\text{O}$  as precursor.

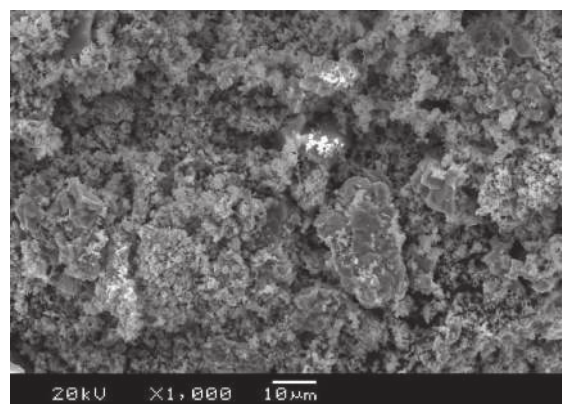


**Figure 6.** SEM image of zirconia nanoparticles synthesized by sol-gel method using  $\text{Zr}(\text{SO}_4)_2 \cdot \text{H}_2\text{O}$  as precursor (non-aqueous medium).

from the sulfate precursor. It appears to be similar to coral shape.

Figure 7 represents the method of preparation of  $\text{ZrO}_2$  nanoparticles from two different precursors, which are chloride and sulphate. The method of preparation is identical in both the cases. However it is interesting to note that their morphology and nanoparticle size are very different, clearly indicating the role of precursors in the synthesis of nanoparticles.

#### 4. Conclusions

Pure zirconium oxide nanoparticles were successfully prepared by sol-gel method. This is a new method used in the synthesis of zirconia nanoparticles in non-aqueous medium. The results clearly indicate that the morphology and size

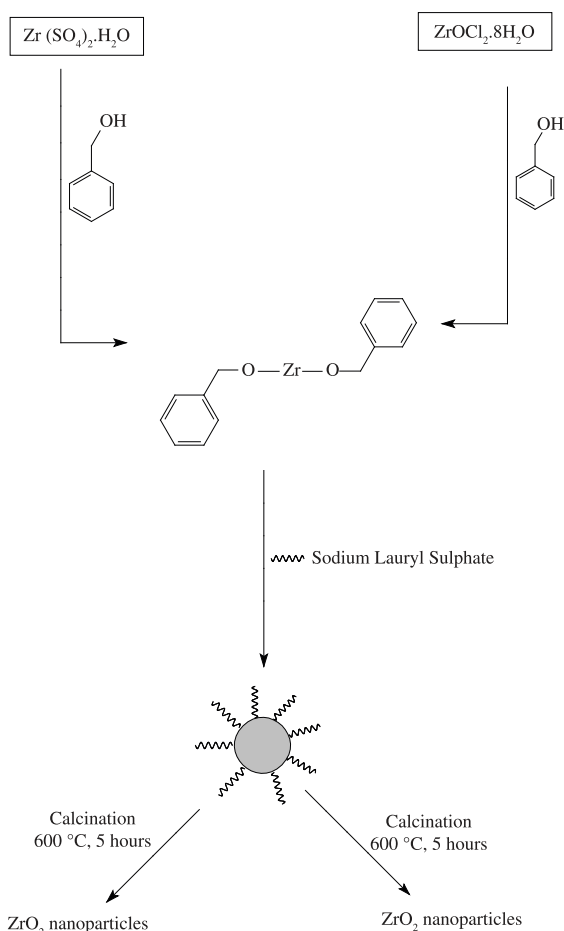


**Figure 7.** Reaction scheme for preparation of  $\text{ZrO}_2$  nanoparticles.

of  $\text{ZrO}_2$  nanoparticles is highly dependent on the precursor used. XRD analysis indicated that the nanoparticles closely resembled and had the tetragonal and monoclinic zirconia nanocrystals. The crystallite size for  $\text{ZrOCl}_2$  precursor was estimated to be 18.1 nm and that from  $\text{Zr}(\text{SO}_4)_2 \cdot \text{H}_2\text{O}$  was 9.7 nm. The TEM results show very different size and shapes for the nanoparticles obtained from the two different precursors.

#### Acknowledgement

This work was supported by King Abdulaziz City for Science and Technology project No. A-18-29 and by the Deanship of Scientific Research, Research Center, College of Science, King Saud University, Riyadh, Kingdom of Saudi Arabia.

#### References

1. Lee WE and Rainforth WM. *Ceramic Microstructures: Property Control by Processing*. London: Chapman & Hall; 1994. p. 317.
2. Juarez RE, Lamas DG, Lascalea GE and Walsoe de Reca NE. Synthesis and Structural Properties of Zirconia-Based Nanocrystalline Powders and Fine-Grained Ceramics. *Defect*

and Diffusion Forum. 1999; 177-178:1-28. <http://dx.doi.org/10.4028/www.scientific.net/DDF.177-178.1>

3. Garvie RC, Hannink RHJ and Pascoe RT. Ceramic steel? *Nature*. 1975; 258:703-5. <http://dx.doi.org/10.1038/258703a0>
4. Heuer AH and Hobbs LW. *Sciences and Technology of Zirconia*. Columbus: American Ceramic Society; 1981. Advances in Ceramics, v. 3.

5. Kalkur TS and Lu YC. Electrical characteristics of ZrO<sub>2</sub>-based metal-insulator-semiconductor structures on p-Si. *Thin Solid Films*. 1992; 207(1-2):193-6. [http://dx.doi.org/10.1016/0040-6090\(92\)90122-R](http://dx.doi.org/10.1016/0040-6090(92)90122-R)
6. Yokoyama T, Setoyama T, Fujita N, Nakajima M, Maki T and Fujii K. Novel direct hydrogenation process of aromatic carboxylic acids to the corresponding aldehydes with zirconia catalyst. *Applied Catalysis A: General*. 1992; 88(2):149-61. [http://dx.doi.org/10.1016/0926-860X\(92\)80212-U](http://dx.doi.org/10.1016/0926-860X(92)80212-U)
7. Stocker C and Baiker A. Zirconia aerogels: effect of acid-to-alkoxide ratio, alcoholic solvent and supercritical drying method on structural properties. *Journal of Non-Crystalline Solids*. 1998; 223(3):165-78. [http://dx.doi.org/10.1016/S0022-3093\(97\)00340-2](http://dx.doi.org/10.1016/S0022-3093(97)00340-2)
8. Stefanc II, Music S, Stefanic G and Gajovic A. Thermal behavior of ZrO<sub>2</sub> precursors obtained by sol-gel processing. *Journal of Molecular Structure*. 1999; 480:621-5. [http://dx.doi.org/10.1016/S0022-2860\(98\)00827-8](http://dx.doi.org/10.1016/S0022-2860(98)00827-8)
9. Wang JA, Valenzuela MA, Salmones J, Vazquez A, Garcia-Ruiz A and Bokhimi X. Comparative study of nanocrystalline zirconia prepared by precipitation and sol-gel methods. *Catalysis Today*. 2001; 68(1-3):21-30. [http://dx.doi.org/10.1016/S0920-5861\(01\)00319-4](http://dx.doi.org/10.1016/S0920-5861(01)00319-4)
10. Srdic VV and Winterer M. Comparison of nanosized zirconia synthesized by gas and liquid phase methods. *Journal of the European Ceramic Society*. 2006; 26(15):3145-51. <http://dx.doi.org/10.1016/j.jeurceramsoc.2005.10.006>
11. Guo G-Y and Chen Y-L. A nearly pure monoclinic nanocrystalline zirconia. *Journal of Solid State Chemistry*. 2005; 178(5):1675-82. <http://dx.doi.org/10.1016/j.jssc.2005.03.005>
12. Wu NL and Wu TF. Enhanced Phase Stability for Tetragonal Zirconia in Precipitation Synthesis. *Journal of the American Ceramic Society*. 2000; 83(12):3225-7. <http://dx.doi.org/10.1111/j.1151-2916.2000.tb01713.x>
13. Vollath D and Sickafus KE. Synthesis of nanosized ceramic oxide powders by microwave plasma reactions. *Nanostructured Materials*. 1992; 1(5):427-37. [http://dx.doi.org/10.1016/0965-9773\(92\)90093-D](http://dx.doi.org/10.1016/0965-9773(92)90093-D)
14. Nitsche R, Rodewald M, Skandan G, Fuess H and Hahn H. Hrtem study of nanocrystalline zirconia powders. *Nanostructured Materials*. 1996; 7(5):535-46. [http://dx.doi.org/10.1016/0965-9773\(96\)00027-X](http://dx.doi.org/10.1016/0965-9773(96)00027-X)
15. Purohit RD, Saha S and Tyagi AK. Combustion synthesis of nanocrystalline ZrO<sub>2</sub> powder: XRD, Raman spectroscopy and TEM studies. *Materials Science and Engineering: B*. 2006; 130(1-3):57-60. <http://dx.doi.org/10.1016/j.mseb.2006.02.041>
16. Meskin PE, Ivanov VK, Barantchikov AE, Churagulov BR and Tretyakov YD. Ultrasonically assisted hydrothermal synthesis of nanocrystalline ZrO<sub>2</sub>, TiO<sub>2</sub>, NiFe<sub>2</sub>O<sub>4</sub> and Ni<sub>0.5</sub>Zn<sub>0.5</sub>Fe<sub>2</sub>O<sub>4</sub> powders. *Ultrasonics Sonochemistry*. 2006; 13(1):47-53. Pmid:16223687. <http://dx.doi.org/10.1016/j.ultsonch.2004.12.002>
17. Lee HY, Iehemann W and Mordike BL. Sintering of nanocrystalline ZrO<sub>2</sub> and zirconia toughened alumina (ZTA). *Journal of the European Ceramic Society*. 1992; 10:245. [http://dx.doi.org/10.1016/0955-2219\(92\)90038-F](http://dx.doi.org/10.1016/0955-2219(92)90038-F)
18. Pecharrmán C, Ocaña M and Serna CJ. Optical constants of tetragonal and cubic zirconias in the infrared. *Journal of Applied Physics*. 1996; 80(6):3479-3483. <http://dx.doi.org/10.1063/1.363218>
19. Gao YF, Masuda Y, Ohta H and Koumoto K. Room-Temperature Preparation of ZrO<sub>2</sub> Precursor Thin Film in an Aqueous Peroxozirconium-Complex Solution. *Chemistry of Materials*. 2004; 16(13):2615-2622. <http://dx.doi.org/10.1021/cm049771i>